Supporting Information:

Correlating Ultrafast Function with Structure in Single Crystals of the Photosynthetic Reaction Center

*Libai Huang,[1,2] Gary P. Wiederrecht,[1] Lisa M. Utschig[2], Sandra Schlesselman,[2] Christina Xydis,[3] Philip D. Laible,[3] Deborah K. Hanson,[3] and David M. Tiede[2]**

Center for Nanoscale Materials[1], Chemical Sciences and Engineering Division[2], and Biosciences Division[3], Argonne National Laboratory, Argonne, IL 60439-4831

*Email: tiede@anl.gov

Experimental Methods

Preparation of reaction center crystals: "Wild-type", polyhistidine-tagged RCs were obtained from a strain of *Rb. sphaeroides* that lacked the light-harvesting II complex. Cells were grown chemoheterotrophically (semi-aerobic, dark, 34 °C).(*1, 2*) RCs were extracted from the cell membranes using the detergent lauryldimethylamine N-oxide (LDAO) and purified using Ni-NTA (nitrilotriacetic acid) immobilized metal affinity chromatography as previously described.(*1, 2*) The detergent LDAO was replaced for octyl β-D-glucopyranoside (OG) by applying the RCs to an anionic exchange column,(*3*) and eluting the RC in a buffer containing 0.8% (w/v) OG, 280 mM NaCl, 10 mM Tris, 1 mM EDTA and pH 7.8. Crystallization in the needle-shaped orthorhombic ($P2_12_12_1$) space group was accomplished by vapor diffusion in the presence of polyethy1ene glycol 4000.(*4-6*)

Ground state absorption spectroscopy: Polarized ground state absorption spectra were acquired by a Nikon TE 200 inverted microscope equipped with an optical spectrograph (HORIBA Jobin Yvon Triax 190) and a liquid nitrogen cooled CCD (HORIBA Jobin Yvon CCD-3500V). A long working distance microscope objective (100x, 6 mm working distance, Mikimoto) was used to focus a halogen white light source to a spot size of ~ 5 μm. Transmitted light was collected by a 20x objective and subsequently detected by the spectrograph and CCD combination. The primary donor in the RC crystals was reduced by 50 mM ascorbic acid before the crystals were positioned within sealed rectangular capillaries with 0.05 mm x 1mm cross-sections (VitroCom).

Transient absorption spectroscopy: The photochemical functions of both RC crystals and detergent-solublized RCs in solution (0.8% n-octyl-β-D-glucopyranoside, 10 mM Tris, pH 7.8) were characterized by ultrafast pump-probe spectroscopy. The experiments were performed with

an amplified Ti:sapphire laser system that outputs 130 fs pulses at 1 kHz as previously described (*9*). The probe pulse was a coherent white light continuum generated by focusing a small fraction (< 1%) of the amplifier output onto a sapphire window. The broadband probe enables transient spectra (by maintaining constant probe delay and scanning a monochromator) or kinetics (by selecting a probe wavelength with a monochromator and scanning the delay line) to be obtained over the visible and near-infrared energies. The primary donor of detergent-solublized RCs was reduced with 50 mM ascorbic acid prior to the measurements. Samples were placed in a 2 mm path length sample cell with an optical density of ~ 1.0 at 800 nm and were bubbled with nitrogen gas. The angle between polarizations of pump and probe beams was fixed at magic angle of 54.7° with a pump power of 150 nJ/pulse with light focused to a spot size of approximately 150 μm. For measurements in crystals, rectangular capillaries containing pre-reduced RC crystals were mounted on a rotating stage and were viewed with a camera. In order to avoid damage to the crystals, the laser pump power was maintained at less than 50 nJ/pulse with light focused to a spot size of approximately 50 μm.

Comparison of Ground-State Absorption and Crystal Coordinate Calculated Transition Moment Projections

Projections for the cofactor optical transition dipole moments onto the orthorhombic crystal $P2_12_12_1$ unit cell **a**, **b**, and **c** axes were calculated using coordinates from the Protein Data Bank entry 4RCR.(*6*) The bacteriochlorophyll and bacteriopheophytin Q_y and Q_x directions were taken as lying along the pyrrole ring I to III and the pyrrole ring II to IV nitrogen-to-nitrogen directions, respectively (*7*). Optical absorption contributed by the transition dipole moment for each cofactor, $A(\lambda) = (\vec{E} \bullet \vec{m})^2 \varepsilon \cdot f(\lambda)$, is the dot product for the unit vectors for the light electric field, $\vec{E}$, and the cofactor transition dipole moment, $\vec{m}$, weighted by the extinction

coefficient, ε, and lineshape function, $f(\lambda)$, . When the light field is aligned along the orthogonal axes of the crystal unit cell, ***a***, ***b***, ***c***, the absorption can be expressed as the extinction coefficient weighted transition dipole projections: $A_{a,b,c}(\lambda) = \cos^2 \vartheta_{a,b,c} \varepsilon \cdot f(\lambda)$. The reaction center $P2_12_12_1$ unit cell was reconstructed from the crystal coordinates using the Cambridge Crystallographic Database Center program Mercury (http://www.ccdc.cam.ac.uk/products/mercury/), and the Q_x and Q_y transition dipole projections, $\cos^2 \vartheta_{a,b,c}$, were calculated for each cofactor in the four reaction center complexes that comprise the unit cell. The calculation confirmed that for the $P2_12_12_1$ symmetry group, each of the four reaction centers in the unit cell makes an equivalent contribution along the unit cell directions. The calculated cofactor transition dipole moment projections were weighted according to their corresponding extinction coefficients (*8*) to provide an crystal coordinate-based index of predicted optical absorption along the unit cell principle axes directions. Figure S1 shows the resulting weighted amplitudes for the BChl and BPh Q_x and Q_y transition moments projected onto **a, b, and c** crystal axis.

Experimental polarized spectra measure along the crystal axes showed pronounced changes in absorption peak positions and amplitudes, although *a priori*, we do not know how the experimentally defined 0^o and 90^o measurement directions correspond to the crystallographic **a**, **b**, **c** directions. The peak shifts are particularly significant since they reflect polarization-resolved contributions of individual transitions within the normally overlapping absorption bands of redundant cofactors in L and M protein subunits. For example, absorption spectra for detergent-solubilized RCs show a single unresolved peak near 540 nm at room temperature that is known to arise from the overlapping Qx absorptions of the BPh_L and BPh_M cofactors absorbing near 542 nm and 530 nm, respectively (*10, 11*). The spectrum measured in crystals

with 0° polarized light shows a BPh Q_x peak at 530 nm that clearly reflects the predominant contribution of BPh_M, while the spectrum recorded with 90° polarized light shows this peak to shift to 540 nm and the flattened shape suggests combined contributions of both BPh_L and BPh_M. The polarized spectra recorded for BPh Q_y transition is found to have a strong preferential absorption 0° polarized light.

We used a comparison of the measured dichroism for the BPh_L and BPh_M cofactors to those calculated from the crystal coordinates to identify the alignment of the unit cell **a**, **b**, **c** directions with respect to the experimental 0^o and 90^o measurement directions. A good agreement was found between experimental polarized absorption spectra (Figure 1a) and patterns for BPh Q_x and Q_y projections along the crystal **a** and **c** directions with 90° and 0° absorption spectra (Figure 1b), respectively. Cofactor projections along the crystal **b** axis showed a pattern that is complementary to the pattern along the **c** axis, with BPh_L making the predominant contribution in the Q_x region and BPh_M making the predominant contribution in the Q_y region (Figure S1). We have also observed crystals exhibiting this ground state absorption pattern as shown in Figure S2, indicating that in different crystals we have measured the RC absorption along each of the principal axes of the $P2_12_12_1$ space group.

Following from this, correlations are also found between the $BChl_L$ and $BChl_M$ Q_y projections and the polarized absorption patterns. $BChl_L$ and $BChl_M$ are known to have overlapping Q_y absorptions that are modeled to have different extents of mixing with transition dipoles and charge transfer states of P, causing the mixed Q_y transitions to be shifted near to 800 nm and 810 nm respectively.(*7, 12-16*) The spectrum recorded with 90° polarized light shows at peak centered at 800 nm that can be expected to reflect an absorption dominated by $BChl_L$. With 0° polarized light the absorption peak shifts to 810 nm and can be understood to be an absorption

dominated by $BChl_M$. The peak positions in the polarized absorption spectra are found to approximately track the expected projection of the $BChl_L$ and $BChl_M$ Q_y directions.

The red-most absorption band arises from the lower energy exciton component of P, P_-, comprised of the Q_y transitions for the two BChl, P_L and P_M , that form P.(*17*) Models have taken into account the effects of coupling between all of the cofactor transition dipoles within the RC and charge transfer states between P_L and P_M.(*7, 12-16*) The polarized spectra recorded for P_- is found to have a strong preferential absorption with light polarized perpendicular to the long axis of the crystal. In addition, the polarized crystal spectra also showed a notable shift in the absorption peak position for P_- that changed from 850 nm in the spectrum recorded with light polarized perpendicular to the long axis of the crystal, to 865 nm when measured with light polarized parallel to the long axis. The polarization-dependent shift in the absorption spectrum of P_- was found to be variable when measured in different crystals with the peak position for P_- measured in the perpendicular polarization ranging from 860 nm to about 848 nm. This peak shift was also found to be reversible. The reversible blue shift in P_- absorption are reminiscent of reversible shifts seen for the absorption of P_- for RCs in different detergent conditions,(*18-21*) and implies that similar changes in the environment surrounding P can occur upon crystallization and subsequent crystal handling.

Primary Charge Separation in Solution

Primary charge separation processes in solution were investigated by femtosecond pump-probe spectroscopy. The excitation wavelength was tuned to 844 nm as shown in Figure 1, which excites primarily the P_- transition. For the measurements of detergent-solubilized RCs in solution, the angle between polarizations of pump and probe beams was fixed at the magic angle of 54.7°. Following excitation, RCs in solution show a rapid, pulse-width limited loss of the Q_x

ground state absorption of P at 595 nm, and slower subsequent loss of the ground state Q_x absorption of BPh_L at 540 nm and concerted growth of the BPh anion band at 650-670 nm that builds in with a 3.7 (±0.3) ps time constant (Figure *S3*). These are well-characterized markers for the formation of the transient $P^+BPh_L^-$ state (*10, 11, 22-24*). In this sample, a slower approximately 100 ps decay is seen on the 665 nm transient that apparently reflects time-evolution of the optical absorption of $P^+BPh_L^-$ and not the depopulation of this state since there is no recovery of the ground state BPh_L Q_x absorption on this time scale. The single wavelength transients measured at 545 nm were fit with a biexponential decay consisting of a 4.5 (± 0.3) ps decay component (90%) combined with a slower 20.0 (± 2.0) ps component (10%). We note that variances in single wavelength kinetics associated with primary electron transfer processes in RCs have been discussed previously (*23*) and that emission decay kinetics from P* also show biphasic kinetics with the major kinetic component reported to be fit with a time constant in the range 2.6 ps to 4.1 ps (*25-27*). Global fitting analyses have been used to provide a self-consistent measure of transient absorption kinetics (*24, 28, 29*). The results presented here demonstrate that the RC solution before crystallization displayed absorbance transients consistent with a 3-4 ps primary electron transfer time to BPh_L.

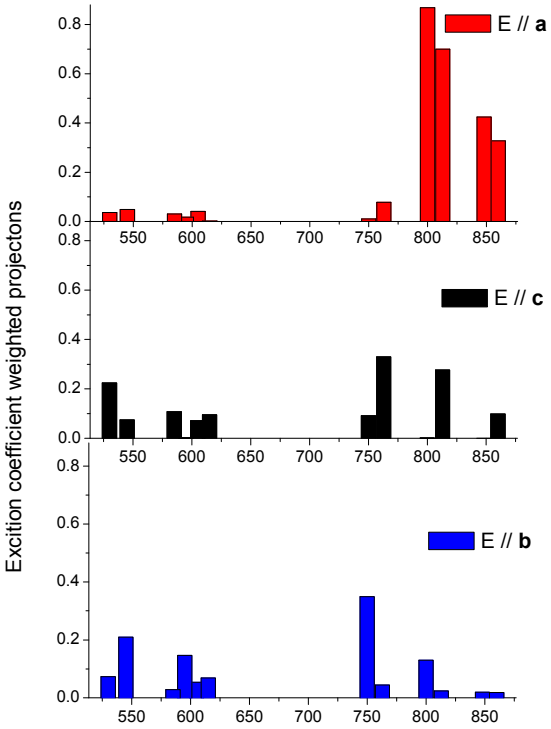

Figure S1. Extinction coefficient weighted projection vectors along **a**, **b** and **c** axis for a single photosynthetic reaction center crystal ($P2_12_12_1$) from *Rb. sphaeroides*.

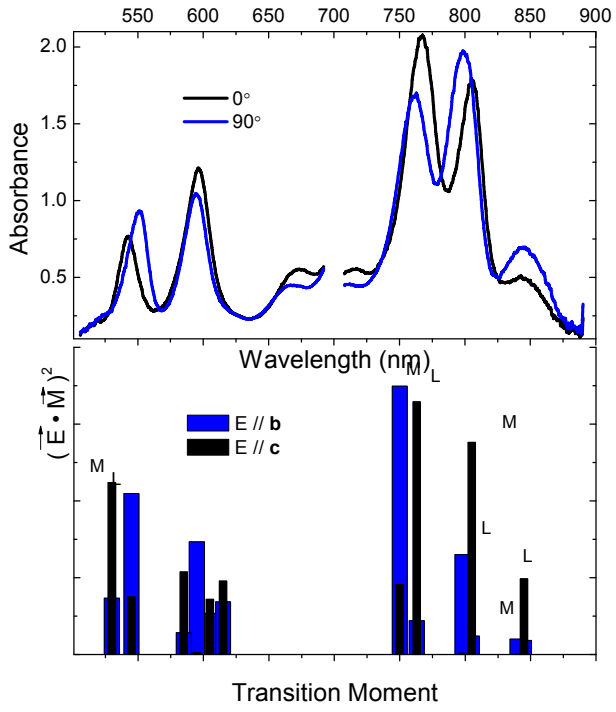

Figure S2. Polarized ground state absorption spectra of a single photosynthetic reaction center crystal ($P2_12_12_1$) from *Rb. sphaeroides*. (a) Spectra with polarized light parallel (red line, 0°) and perpendicular (black line, 90°) to the long axis of the crystal, respectively. (b) Extinction coefficient weighted projection vectors along **b** and **c** axis.

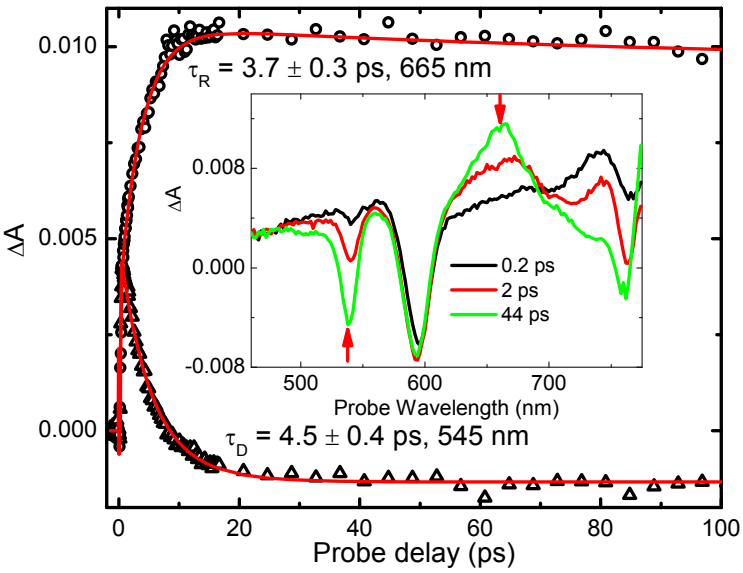

Figure S3. Transient absorption spectra (insets) and kinetics of detergent-solubilized RCs. Kinetic traces were taken at 545 nm (open triangles) and 665 nm (open circles). The red solid lines are biexponential fits convoluted with the pump pulse with time constants resulted from the fits indicated in the figures. The RC (20 μM) were suspended in a solution containing 0.8% n-octyl-β-D-glucopyranoside, 10 mM Tris, pH 7.8, and 50 mM sodium ascorbate.

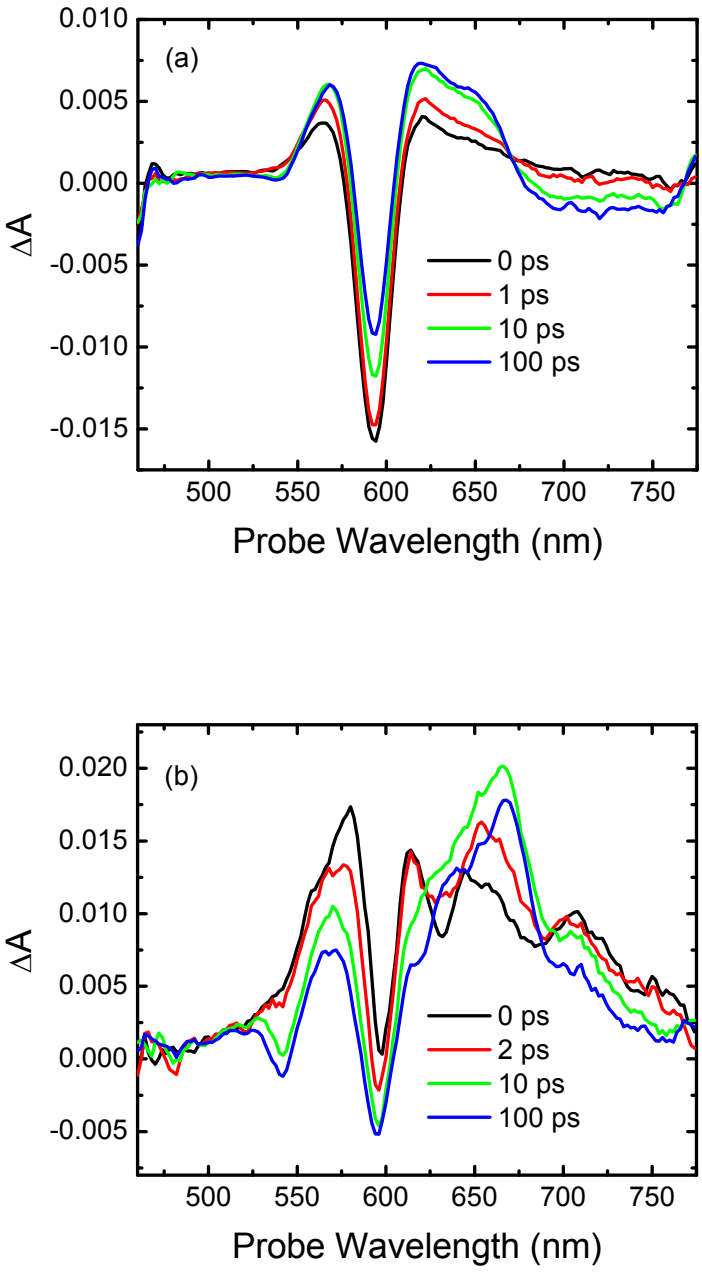

Figure S4. Transient absorption spectra of a single RC crystal. Polarizations of pump was perpendicular to the long axis (90°) and probe polarization was either parallel (0°) (a) or perpendicular (90°) (b) to the long axis of the crystal.

.

References:

1. Pokkuluri, P. R., Laible, P. D., Deng, Y. L., Wong, T. N., Hanson, D. K., and Schiffer, M. (2002) The structure of a mutant photosynthetic reaction center shows unexpected changes in main chain orientations and quinone position, *Biochemistry 41*, 5998-6007.
2. Kirmaier, C., Bautista, J. A., Laible, P. D., Hanson, D. K., and Holten, D. (2005) Probing the contribution of electronic coupling to the directionality of electron transfer in photosynthetic reaction centers, *Journal of Physical Chemistry B 109*, 24160-24172.
3. Tiede, D. M., Vazquez, J., Cordova, J., and Marone, P. A. (1996) Time-resolved electrochromism associated with the formation of quinone anions in the Rhodobacter sphaeroides R26 reaction center, *Biochemistry 35*, 10763-10775.
4. Chang, C. H., Schiffer, M., Tiede, D., Smith, U., and Norris, J. (1985) Characterization of Bacterial Photosynthetic Reaction Center Crystals from Rhodopseudomonas-Sphaeroides R-26 by X-Ray-Diffraction, *Journal of Molecular Biology 186*, 201-203.
5. Chang, C. H., Tiede, D., Tang, J., Smith, U., Norris, J., and Schiffer, M. (1986) Structure of Rhodopseudomonas-Sphaeroides R-26 Reaction Center, *Febs Letters 205*, 82-86.
6. Yeates, T. O., Komiya, H., Chirino, A., Rees, D. C., Allen, J. P., and Feher, G. (1988) Structure of the Reaction Center from Rhodobacter-Sphaeroides R-26 and 2.4.1-Protein-Cofactor (Bacteriochlorophyll, Bacteriopheophytin, and Carotenoid) Interactions .4, *Proceedings of the National Academy of Sciences of the United States of America 85*, 7993-7997.
7. Parson, W. W., and Warshel, A. (1987) Spectroscopic Properties of Photosynthetic Reaction Centers .2. Application of the Theory to Rhodopseudomonas-Viridis, *Journal of the American Chemical Society 109*, 6152-6163.
8. Straley, S. C., Parson, W. W., Mauzerall, D. C., and Clayton, R. K. (1973) Pigment content and molar extinction coefficients of photochemical reaction centers from Rhodopseudomonas spheroides, *Biochim Biophys Acta 305*, 597-609.
9. Greenfield, S. R., and Wasielewski, M. R. (1995) Optical Parametric Amplification of Femtosecond Pulses Tunable from the Blue to the Infrared with Microjoule Energies, *Applied Optics 34*, 2688-2691.
10. Kirmaier, C., and Holten, D. (1987) Primary photochemistry of reaction centers from photosyntheic purple bacteria, *Photosynth. Res. 13*, 225-260.
11. Kirmaier, C., Holten, D., and Parson, W. W. (1985) Picosecond-photodichroism studies of the transient states in *Rhodopseudomonas sphaeroides* reaction centers at 5K. Effects of electron transfer on the six bacteriochlorin pigments, *Biochim. Biophys. Acta 810*, 49-61.
12. Warshel, A., and Parson, W. W. (1987) Spectroscopic Properties of Photosynthetic Reaction Centers .1. Theory, *Journal of the American Chemical Society 109*, 6143-6152.
13. Thompson, M. A., and Zerner, M. C. (1991) A Theoretical-Examination of the Electronic-Structure and Spectroscopy of the Photosynthetic Reaction Center from Rhodopseudomonas-Viridis, *Journal of the American Chemical Society 113*, 8210-8215.
14. Lathrop, E. J. P., and Friesner, R. A. (1994) Simulation of Optical-Spectra from the Reaction-Center of Rhodobacter-Sphaeroides - Effects of an Internal Charge-Separated State of the Special Pair, *Journal of Physical Chemistry 98*, 3056-3066.

15. Zhou, H. L., and Boxer, S. G. (1997) Charge resonance effects on electronic absorption line shapes: Application to the heterodimer absorption of bacterial photosynthetic reaction centers, *Journal of Physical Chemistry B 101*, 5759-5766.
16. Chang, C. H., Hayashi, M., Liang, K. K., Chang, R., and Lin, S. H. (2001) A theoretical analysis of absorption spectra of photosynthetic reaction centers: Mechanism of temperature dependent peak shift, *Journal of Physical Chemistry B 105*, 1216-1224.
17. Jonas, D. M., Lang, M. J., Nagasawa, Y., Joo, T., and Fleming, G. R. (1996) Pump-Probe Polarization Anisotropy Study of Femtosecond Energy Transfer within the Photosynthetic Reaction Center of Rhodobacter sphaeroides R26, *J. Phys. Chem. 100*, 12660-12673.
18. Wang, S., Lin, S., Lin, X., Woodbury, N. W., and Allen, J. P. (1994) Comparative-Study of Reaction Centers from Purple Photosynthetic Bacteria - Isolation and Optical Spectroscopy, *Photosynthesis Research 42*, 203-215.
19. Gast, P., Hemelrijk, P. W., VanGorkom, H. J., and Hoff, A. J. (1996) The association of different detergents with the photosynthetic reaction center protein of Rhodobacter sphaeroides R26 and the effects on its photochemistry, *European Journal of Biochemistry 239*, 805-809.
20. Muh, F., Rautter, J., and Lubitz, W. (1997) Two distinct conformations of the primary electron donor in reaction centers from Rhodobacter sphaeroides revealed by ENDOR/TRIPLE-spectroscopy, *Biochemistry 36*, 4155-4162.
21. Palazzo, G., Carbone, L., Colafemmina, G., Angelieo, R., Ceglie, A., and Giustini, M. (2004) The role of the cosurfactant in the CTAB/water/n-pentanol/n-hexane system: Pentanol effect on the phase equilibria and mesophase structure, *Physical Chemistry Chemical Physics 6*, 1423-1429.
22. Fajer, J., Brune, D. C., Davis, M. S., Forman, A., and Spaulding, L. D. (1975) Primary charge separation in bacterial photosynthesis: oxidized chlorophylls and reduced pheophytin, *Proc. Natl. Acad. Sci. U.S.A. 72*, 4956-4960.
23. Kirmaier, C., and Holten, D. (1990) Evidence that a distribution of bacterial reaction centers underlies the temperature and detection-wavelength dependence of the rates of primary electron-transfer reactions, *Proc. Natl. Acad. Sci. USA 87*, 3552-3556.
24. Holzwarth, A. R., and Müller, M. G. (1996) Energetics and kinetics of radical pairs in reaction centers from *Rhodobacter sphaeroides*. A femtosecond transient absorption study, *Biochemistry 35*, 11820-11831.
25. Vos, M. H., Lambry, J. C., Robles, J. C., Youvan, D. C., Breton, J., and Martin, J.-L. (1991) Direct observation of vibrational coherence in bacterial reaction centers using femtosecond absorption spectroscopy, *Proc. Natl. Acad. Sci. USA 88*, 8885-8889.
26. Du, M., Rosenthal, S. J., Xie, X., DiMagno, T. J., Schmidt, M., Hanson, D. K., Schiffer, M., Norris, J. R., and Fleming, G. R. (1992) Femtosecond spontaneous-emission studies of reaction centers from photosynthetic bacteria, *Proc. Natl. Acad. Sci. U.S.A. 89*, 8517-8521.
27. Peloquin, J. M., Lin, S., Taguchi, A. K. W., and Woodbury, N. W. (1995) Excitation wavelength dependence of bacterial reaction center photochemistry. 1. Ground state and excited state evolution, *J. Phys. Chem. 99*, 1349-1356.
28. van Brederode, M. E., van Stokkum, I. H. M., Katilius, E., van Mourik, F., Jones, M. R., and van Grondelle, R. (1999) Primary charge separation routes in the BChI : BPhe

heterodimer reaction centers of Rhodobacter sphaeroides (vol 38, pg 7545, 1999), *Biochemistry 38*, 9556-9556.

29. van Stokkum, I. H. M., Beekman, L. M. P., Jones, M. R., van Brederode, M. E., and van Grondelle, R. (1997) Primary electron transfer kinetics in membrane-bound Rhodobacter sphaeroides reaction centers: A global and target analysis, *Biochemistry 36*, 11360-11368.